CFD SIMULATION OF THERMAL PLUME AND FIREBRANDS SCATTERING IN URBAN FIRE

HONG HUANG[1], RYOZO OOKA[1], SHINSUKE KATO[1],
HIROSHI OTAKE[2] AND YOSHIHIKO HAYASHI[3]
[1]Institute of Industrial Science, University of Tokyo, Japan
[2]Department of Architecture Engineering, University of Tokyo, Japan
[3] Building Research Institute, Japan

ABSTRACT

Firebrand is found to be an important fire spread factor in large urban fire. In this study, the scattering of firebrands in an urban fire was numerically simulated by means of CFD (Computation Fluid Dynamics). Firstly, thermal plume of the urban fire was predicted using a modified compressible k- ε turbulent model which was verified by fire tunnel experiment. Then a Lagrangian trajectory model considering drag force, pressure force and gravity force of firebrands was applied to predict the trajectory of firebrands. The influences of inflow wind velocity, diameter, generating site, initial generating velocity were investigated. It is found that when inflow wind velocity is comparatively low, the thermal plume is significant, and when the inflow wind is strong, the thermal plume is suppressed. It is shown that the smaller the diameter of firebrand is and the stronger the fire thermal plume is, the farther it may be scattered. Increasing the initial generating velocity can make the firebrands fly farther.

1. INTRODUCTION

Firebrands scattering by the wind is an important factor in urban fire spread as well as the radiation and convection from the fire thermal plume. From the investigation of past urban fires, fire spread due to firebrands almost occurred, especially in the case of large damage fire. Therefore, the prediction of the firebrands scattering in large scale urban fire or simultaneous occurrence fire during earthquake is strongly expected. However, there is little finding about the physical process of firebrands for its difficulty in too many uncertainties, such as meteorology conditions, the combustion situation of fire buildings, the type of building materials et al. Some researches have been done to predict the maximum firebrands flying distance in forest fire. A simple semi-experimental model was applied to predict the fire thermal plume and Lagrangian equation was used to calculate the trajectories of firebrands by Albini (1979). Morris (1987) developed a method to simplify the Albini's model. However, little research has been down for the firebrand in urban fire. It is known that the wind can greatly affect the trajectories of firebrands. Therefore, because of the existence of buildings, the wind should be predicted precisely in the urban space as possible. The CFD (Computational Fluid Dynamics) is thought to

be a good approach to reach the aim. Shiraishi et al (2001) simulated the firebrands scattering in urban fire by means of CFD. They treated firebrands as airborne particles. This is effective for small diameter firebrands, however it has limitation when predicting large diameter firebrands.

In this study, in order to prediction the firebrands scattering, the following CFD (Computational Fluid Dynamics) approach has been applied. Firstly, fire thermal plume is predicted in urban fire using a modified compressible k-ε turbulent model, secondly, the Lagrangian transport equation of firebrands is solved considering the forces on firebrands, such as gravity, drag force and pressure force.

2. MODEL DESCRIPTION

2.1 The gas-phase model

The flow is described by the three-dimensional, Faver-averaged equations of transport for mass, momentum, enthalpy and gas species. Table 1 shows the governing equations. Turbulence is modeled using a modified k-ε model, which is proposed by El Tahry (1983) for compressible reciprocating engine flows. The main difference between the modified model with common model is the last term of ε equation (Equation 6) which results from compressibility effects.

Table 1: The governing equations

$$\frac{\partial \overline{\rho}}{\partial t}+\frac{\partial(\overline{\rho}\widetilde{u}_j)}{\partial x_j}=0 \qquad (1)$$

$$\frac{\partial(\overline{\rho}\widetilde{u}_i)}{\partial t}+\frac{\partial}{\partial x_j}(\overline{\rho}\widetilde{u}_i\widetilde{u}_j)=-\frac{\partial \overline{p}}{\partial x_i}+\frac{\partial}{\partial x_j}(\overline{\tau}_{ij}-\overline{\rho}\widetilde{u_i''u_j''})+\overline{\rho}g_i \qquad (2)$$

$$\frac{\partial(\overline{\rho}\widetilde{h})}{\partial t}+\frac{\partial}{\partial x_j}(\overline{\rho}\widetilde{u}_j\widetilde{h})=\frac{\partial \overline{p}}{\partial t}+\frac{\partial}{\partial x_j}(\frac{\lambda}{c_p}\frac{\partial \widetilde{h}}{\partial x_j}-\overline{\rho}\widetilde{u_i''h''}+\sum_{n=1}^{N}\overline{h}_n\overline{\rho}D_n\frac{\partial \widetilde{Y}_n}{\partial x_j})+\overline{u}_j\frac{\partial \overline{p}}{\partial x_j}+\overline{\tau}_{ij}\frac{\partial \overline{u}_i}{\partial x_j}-\overline{S}_R \qquad (3)$$

$$\frac{\partial(\overline{\rho}\widetilde{Y}_n)}{\partial t}+\frac{\partial}{\partial x_j}(\overline{\rho}\widetilde{u}_j\widetilde{Y}_n)=\frac{\partial}{\partial x_j}(\overline{\rho}D_n\frac{\partial \widetilde{Y}_n}{\partial x_j}-\overline{\rho}\widetilde{u_i''Y_n''})+\overline{w}_n \qquad (4)$$

$$\frac{\partial(\overline{\rho}\widetilde{k})}{\partial t}+\frac{\partial(\overline{\rho}\widetilde{u}_j\widetilde{k})}{\partial x_j}=\frac{\partial}{\partial x_j}((\frac{\mu+\mu_t}{\sigma_k})\frac{\partial \widetilde{k}}{\partial x_j})+\mu_t(\frac{\partial \widetilde{u}_i}{\partial x_j}+\frac{\partial \widetilde{u}_j}{\partial x_i})\frac{\partial \widetilde{u}_i}{\partial x_j}-\frac{2}{3}(\mu_t\frac{\partial \widetilde{u}_k}{\partial x_k}+\overline{\rho}\widetilde{k})\frac{\partial \widetilde{u}_i}{\partial x_i}-g_i\frac{\mu_t}{\sigma_{h,t}}\frac{1}{\overline{\rho}}\frac{\partial \overline{\rho}}{\partial x_i}-\overline{\rho}\widetilde{\varepsilon} \qquad (5)$$

$$\frac{\partial(\overline{\rho}\widetilde{\varepsilon})}{\partial t}+\frac{\partial(\overline{\rho}\widetilde{u}_j\widetilde{\varepsilon})}{\partial x_j}=\frac{\partial}{\partial x_j}((\frac{\mu+\mu_t}{\sigma_\varepsilon})\frac{\partial \widetilde{\varepsilon}}{\partial x_j})+$$
$$C_{\varepsilon 1}\frac{\widetilde{\varepsilon}}{\widetilde{k}}(\mu_t(\frac{\partial \widetilde{u}_i}{\partial x_j}+\frac{\partial \widetilde{u}_j}{\partial x_i})\frac{\partial \widetilde{u}_i}{\partial x_j}-\frac{2}{3}(\mu_t\frac{\partial \widetilde{u}_k}{\partial x_k}+\overline{\rho}\widetilde{k})\frac{\partial \widetilde{u}_i}{\partial x_i}+C_{\varepsilon 3}\max(g_i\frac{\mu_t}{\sigma_h}\frac{1}{\overline{\rho}}\frac{\partial \overline{\rho}}{\partial x_i},0))-C_{\varepsilon 2}\overline{\rho}\frac{\widetilde{\varepsilon}^2}{\widetilde{k}}+C_{\varepsilon 4}\overline{\rho}\widetilde{\varepsilon}\frac{\partial \widetilde{u}_i}{\partial x_i} \qquad (6)$$

$$h=\sum_{n=1}^{N}Y_nh_n=\sum_{n=1}^{N}Y_n(h_{0,n}+\int_{T_0}^{T}c_{p,n}dT) \qquad (7) \qquad \overline{\rho}=\frac{\overline{p}}{R\sum_{n=1}^{N}(\frac{\widetilde{T}\widetilde{Y}_n}{M_n})} \qquad (8)$$

$$\overline{\tau}_{ij}=\mu(\frac{\partial \overline{u}_i}{\partial x_j}+\frac{\partial \overline{u}_j}{\partial x_i}-\frac{2}{3}\frac{\partial \overline{u}_k}{\partial x_k}\delta_{ij}) \qquad (9) \qquad \overline{\rho}\widetilde{u_i''u_j''}=-\mu_t(\frac{\partial \widetilde{u}_i}{\partial x_j}+\frac{\partial \widetilde{u}_j}{\partial x_i})+\frac{2}{3}(\mu_t\frac{\partial \widetilde{u}_k}{\partial x_k}+\overline{\rho}\widetilde{k})\delta_{ij} \qquad (10)$$

$$\overline{\rho}\widetilde{u_j''h''}=-\frac{\mu_t}{\sigma_h}\frac{\partial \widetilde{h}}{\partial x_j} \qquad (11) \qquad \overline{\rho}\widetilde{u_j''Y_n''}=-\frac{\mu_t}{\sigma_n}\frac{\partial \widetilde{Y}_n}{\partial x_j} \qquad (12)$$

$\sigma_k=1.0,\quad \sigma_\varepsilon=1.22,\quad \sigma_h=0.7,\quad \sigma_n=0.7,\quad C_{\varepsilon 1}=1.44,\quad C_{\varepsilon 2}=1.92,\quad C_{\varepsilon 3}=1.44,\quad C_{\varepsilon 4}=-0.33$

$n=$ *fuel*, *oxygen*, *product*

Combustion in the gaseous phase is modeled using the eddy break up model (Magnussen, 1976) here, which is widely used in fire modeling6). The reaction rate is determined by the slowest of the turbulence dissipation rates of either fuel or oxygen, i.e.,

$$\overline{w}_f=-\overline{\rho}(\varepsilon/k)\min(A\widetilde{Y}_f,A\widetilde{Y}_{O_2}/i) \qquad (13)$$

Where A takes the value 4.0, i is the stoichiometric ratio of oxygen to fuel,

respectively. The following chemical reaction is assumed (Novozhilov, 1996):

$$C_nH_m + (n - s + \frac{m}{4})(O_2 + 3.76N_2) \rightarrow sC + (n-s)CO_2 + \frac{m}{2}H_2O + 3.76(n - s + \frac{m}{4})N_2 \quad (14)$$

Here s is a parameter to define the amount of soot produced. A non-zero value results in some of the carbon remaining as soot, with a consequent reaction to CO2. s can be decided from soot conversion factor which is chosen from some experiments data, for example, 2% for propane (Yan, 1996, Tewarson, 1995). The soot concentration is determined from the species equation and treated as a gas-phase species.

Radiation is solved here paralleling with the governing equations. The discrete transfer method (Lockwood, 1981) is used to provide the radiation source term for the energy equation of the gas phase and the radiation flux to the solid surface. The absorption and emission of gas and soot are also considered. The effect on radiation intensity is presented by following equation.

$$\frac{dI}{ds} = -(k_g + k_s)I + \frac{\sigma}{\pi}(k_g + k_s)T^4 \quad (15)$$

Scattering is negligible due to the small diameter of soot. The absorption coefficients of gas and soot (Equation 16, 17) presented by Novozhilov et al (1997) are used, and the soot density is assumed to be 2000kg/m3 for the soot volume fraction (fv) calculation (Jia, 1998, Fairwather, 1992).

$$k_g = 0.28\exp(-\frac{T}{1135}), \quad (16) \qquad k_s = 1264\ f_v T \quad (17)$$

The solution of the equations is based on finite volume method. Convection terms are discretised using upwind differencing scheme. The SIMPLE pressure correction algorithm is used. The gas-phase model was verified by a fire tunnel experiment which was performed by Hayashi et al. (2002) in order to study the fire plume characteristic in urban fire.

2.2 Firebrands model

Firebrands are thought to be sphere, and the behavior of firebrands in the air flow can be considered to be air-solid two phase flow. Therefore, the scattering of firebrands can be presented by Lagrangian transport equation. From the DNS analysis of Rouson & Eaton (1997), virtual mass force, lift force and buoyance force may be ignored when the solid particle scale is smaller than the minimum length scale of turbulent flow and it is very smaller compared with the density of the gas. Then we can obtain following momentum equation.

$$m_d \frac{d\vec{u}_d}{dt} = \vec{F}_{dr} + \vec{F}_p + \vec{F}_g \quad (18)$$

$\vec{F}_g = (\mathrm{m_p}\vec{\mathrm{g}}(\vec{\mathrm{g}} = (0,0,\text{-}9{,}8)\mathrm{m/s^2}))$ is the gravity. Drag force $\vec{F}_{dr}$ is given by

$$\vec{F}_{dr} = \frac{1}{2}C_d \rho A_d \,|\vec{u} - \vec{u}_d\,|(\vec{u} - \vec{u}_d) \quad (19)$$

$\vec{F}_p$ is the pressure force given by

$$\vec{F}_p = -V_d \nabla p \quad (20)$$

Drag coefficient C_d is calculated using the following expression:

$$C_d = \begin{cases} 24(1 + 0.15\,\mathrm{Re}_d^{0.687})/\mathrm{Re}_d, & \mathrm{Re}_d \le 10^3 \\ 0.44, & \mathrm{Re}_d > 10^3 \end{cases} \quad (21)$$

where, Red is the Reynolds number of the firebrand.

$$\mathrm{Re}_d = \frac{\rho\,|\vec{u} - \vec{u}_d|\,D_d}{\mu} \quad (22)$$

3. SIMULATION DESCRIPTION

3.1 Simulation model

The urban wind becomes very complex due to the complexity of the urban buildings. A simplified urban model is used here, which includes three blocks having a interval of 100m. A building is assumed to be in fire. Figure 1 shows the urban model with a analytical area of 370m(X) × 110m(Y) ×160m(Z). The height of the building is assumed to be 10m as well as the width and the depth. The interval between buildings in one block is also assumed to be 10m. The firebrands are assumed to be generated from 81 points over the roof averagely. They are shown in Figure 2, the interval between points is 1.0m.

3.2 Simulation cases and boundary conditions

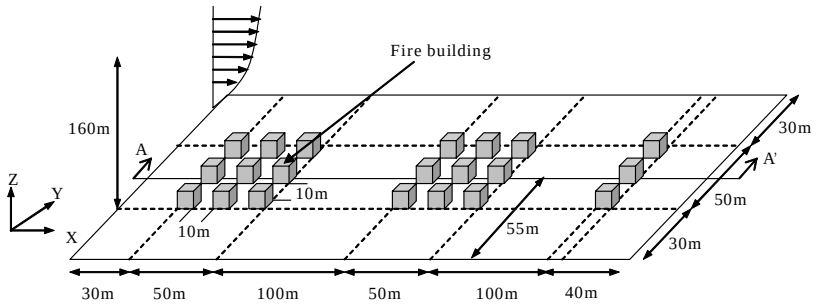

Figure 1: Simulation domain

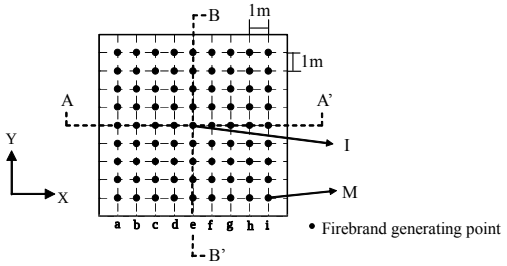

Figure 2: Firebrands generating points

Table 2 and Table 3 show the simulation cases and boundary conditions, respectively. Two kinds of inflow wind velocity are chosen in which fire spread due to firebrands often occurred from previous report. There is little data about the density of firebrands, it is estimated from some experiment data (Yoshioka, 2003) here. The initial velocity is set to be the same value which is close to the wind velocity of the fire face at all generation points. The effect of the change of Z direction initial velocity is also considered. The fuel is injected to the air to reach a heat release of

2.0MW/m^2. A computational grid of 145 cells along the tunnel, 45 cells across and 35 cells in the vertical direction is used.

Table 2:Simulation cases

Case	Inflow Velocity (m/s)	Firebrands properties			
		Density (kg/m^3)	Diameter (cm)	Initial Velocity (m/s)	
				X	Z
1	5.0	30	1	5.0	2.0
2	5.0	30	1	5.0	5.0
3	5.0	30	1.5	5.0	2.0
4	5.0	30	1.5	5.0	5.0
5	5.0	30	2	5.0	2.0
6	5.0	40	1	5.0	2.0
7	5.0	40	1	5.0	5.0
8	5.0	40	1.5	5.0	2.0
9	10.0	30	1	5.0	2.0
10	10.0	30	1.5	5.0	2.0

Table 3:Boundary condition

Inlet	$U_1(x_3)/U_D=(x_3/D)^{1/4}$,$U_2(x_3)=0$,$U_3(x_3)=0$, $\varepsilon(x_3)=C_\mu k(x_3)^{3/2}/l(x_3)$, $l(x_3)=4(C_\mu k(x_3))^{1/2}D^{1/4}x_3^{3/4}/U_D$, k: Experiemntal data (Murakmi, 1988)
Outlet, sky, side	free slip
Wall surface	Logarithm function q=2.0MW/m^2 at fire face

4. RESULTS AND DISCUSSION

4.1 Wind velocity and temperature distribution in urban fire

The vertical wind velocity distributions for the two inflow wind velocity of section A-A' (Figure 1) are shown in Figure 3 and 4 respectively. The vertical temperature distributions are shown in Figure 5 and Figure 6. When the inflow wind velocity is 5.0m/s, the thermal plume is strong and reaches up to about 30m height, when the inflow wind velocity is 10.0m/s, the thermal plume is suppressed and greatly inclines at the leeward side which increases the risk of fire spread to the close buildings. The horizontal temperature distributions at 10.0m height are shown in Figure 7 and Figure 8. The diffusion range of temperature is wider in the case of inflow wind velocity 10.0m/s than the one of 5.0m/s. It is found that the high temperature region diverges to the leeward side and symmetry is seen, and the temperature is suppressed in the center line. It is thought that the circling flow formed after the building suppresses the convection and diffusion of the temperature in the center line.

4.2 Firebrands trajectories

The vertical and horizontal trajectories of firebrands (case 1, 7, 9) are shown in Figure 9-14. The firebrands can fly over 200m and reach up to 30m high. In the same air flow, we can see the tendency that the heavier the

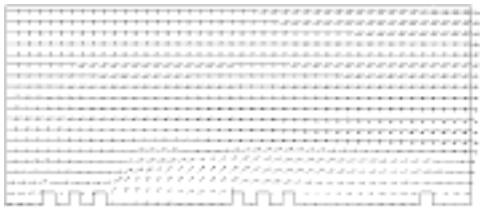

Figure 3: Wind distribution (U_D=5.0m/s)→ 5.0m/s

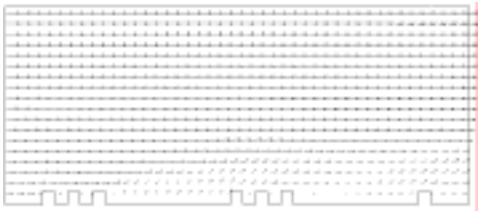

Figure 4: Wind distribution (U_D=10.0m/s)→ 10m/s

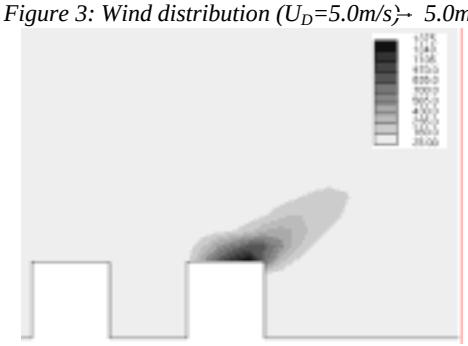

Figure 5: Vertical temperature distribution (ºC) (U_D=5.0m/s)

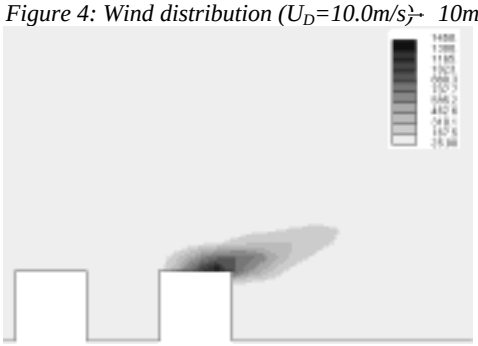

Figure 6: Vertical temperature distribution (ºC) (U_D=10.0m/s)

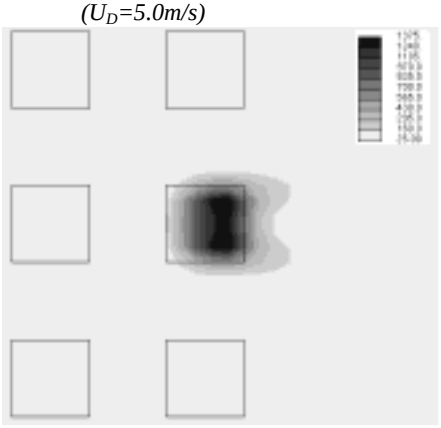

Figure 7: Horizontal temperature distribution (ºC) (U_D=5.0m/s, Height=10.0m)

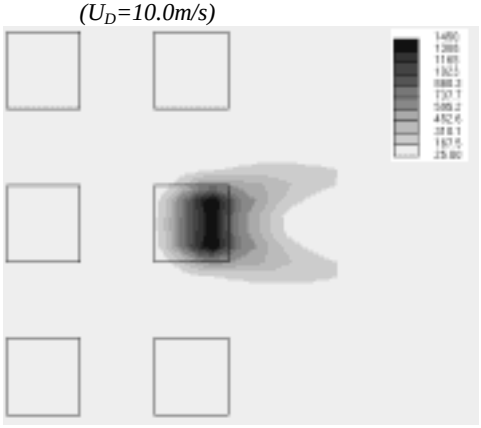

Figure 8: Horizontal temperature distribution (ºC) (U_D=10.0m/s, Height=10.0m)

firebrands are, the farther they can fly in X direction, and the lighter the firebrands are, the wider they can be scattered in Y direction comparing with case 1 (density: 30kg/m3) and case 7 (density: 40kg/m3). The firebrands can not fly over 30.0m in the case 5 (density: 30kg/m3, diameter: 2cm) and case 8 (density: 40kg/m3, diameter: 1.5cm) for the heavy mass. When the inflow wind velocity is higher, the possibility of flying higher is raised, however the scattering in Y direction is decreased.

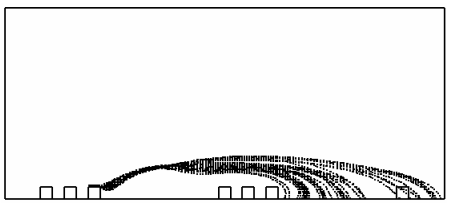

Figure 9: Vertical trajectories of firebrands (case 1)

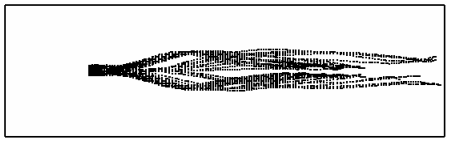

Figure 10: Horizontal trajectories of firebrands (case 1)

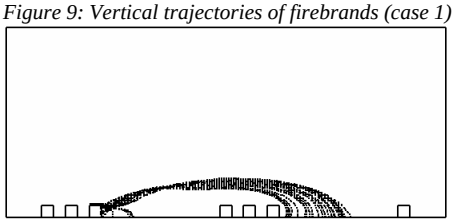

Figure 11: Vertical trajectories of firebrands (case 7)

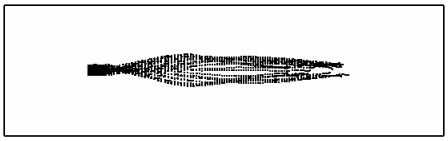

Figure 12: Horizontal trajectories of firebrands (case 7)

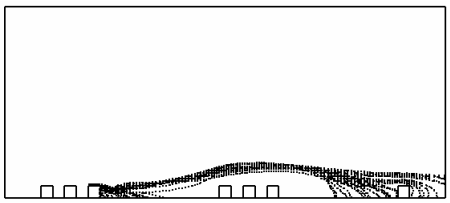

Figure 13: Vertical trajectories of firebrands (case 9)

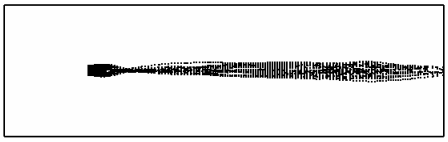

Figure 14: Horizontal trajectories of firebrands (case 9)

4.2.1 *Ratios of firebrands for different flying distances*

Figure 15 shows the ratios of firebrands depending on the X direction flying distance. The 0-10m means the firebrands almost can't fly out of the building. The heaver the firebrands are, the ratio of not out of the building is high. It reaches 58% for case 3 (density: 30kg/m3, diameter:1.5cm). Case 2 and case 7, which is the cases that the Z direction initial generating velocity (W_{int}) is raised to 5.0m/s, show lowest ratios here. This means that the increasing of W_{int} can make the firebrands fly further. Except the ones not flying out of the building, the flying distances are concentrate in 100-200m when the inflow wind velocity is 5.0m/s. Contrast to the case of 0-10m, case 2 and case 7 show higher ratios. When the inflow wind velocity is 10.0m/s, most firebrands fly a distance in 200-300m.

4.2.2 *The characters of firebrands generated from different sites*

Maximum X direction flying distance is shown in Figure 16 for different starting line. The starting line is shown in Figure 2. The starting line where the firebrands begin to fly out the building, i.e. the flying distance is over 10.0m, is checked. The differences between case 1, 2 and case 6, 7 imply that increasing the W_{int} can make the line moves to windward. Increasing the mass of firebrands makes the line moves to leeward from the difference between case 1, 3 and 6.

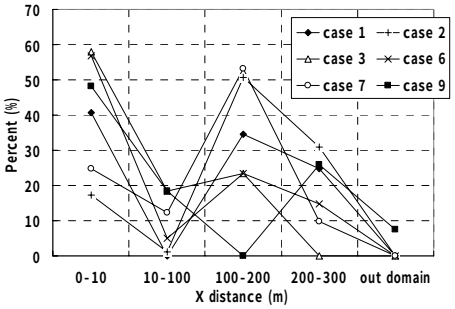

Figure 15 Ratios of firebrands depending on the X direction flying distance

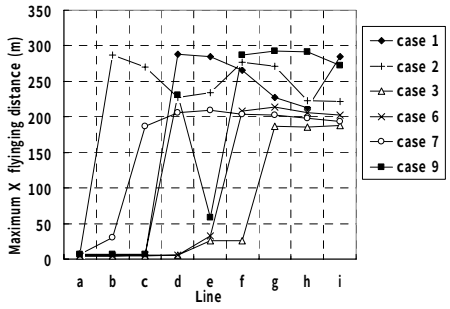

Figure 16 Maximum X direction flying distance depending on the starting line

5. CONCLUSION

CFD simulation has been carried out in the present work to study the scattering of firebrands in an urban fire. Firstly, thermal plume of the urban fire was predicted using a modified compressible k-ε turbulent model. Then a Lagrangian trajectory model considering drag force, pressure force and gravity force of firebrands was applied to predict the trajectory of firebrands.

It is found that when inflow wind velocity is comparatively low, thermal plume is significant, and when it is a strong wind, thermal plume is suppressed but the fire spread risk to the leeward building is increased. The temperature in the center line is suppressed due to the formation of the circle flow after the building. It is shown that the smaller the diameter of firebrand is and the stronger the fire thermal plume is, the further it may be scattered. Increasing the Z direction initial generating velocity can make the firebrands fly farther. The more leeward side the firebrands are generated in the fire, the more easier they can be scattered.

ACKNOWLEDGEMENT

A part of this work was supported by the scientific research fund: Basic B (Study on the mechanism of fire spread due to firebrands in urban fire by fire tunnel experiment and CFD simulation, Project leader: Dr. Y. Hayashi), which is gratefully acknowledged.

REFERENCES

Albini, F. A., 1979, USDA Forest Service, General Technical Report, INT-56.

Bilger, R. W., 1995, In Proc. 4th Int. Symp. on Fire Safety Science, 95-110.

EI Tahry, S. H., 1983, AIAA, J. Energy, 7, 4, 345-353.

Fairweather, M., Jones, W. P. & Lindstedt, R. P., 1992, Combustion Flame, 89, 45-63.

Hayashi, Y., Saga, T., Suzuki, K. & Wakamatsu, T., 2002, Summaries of Technical Papers of Annual Meeting of Architecture Institute of Japan, 297-300.

Jia, F., Galea, E. R. & Patel, M. K., 1998, J. Applied Fire Science, 8, 4, 327-352.

Lockwood, F. C. & Shah, N. G., 1981, 18th Symposium (International) on Comubusition, 1405-1414.

Magnussen, B. F. & Hjertager, H., 1976, In Proceedings 16th Symposium (International) on Combustion, The Combustion Institute, Pittsburgh, 719-729.

Morris, G. A., 1987, USDA Forest Service, Research Note, INT-374.

Murakami, S., Mochida, A. & Hayashi, Y., 1988, 10th wind engineering symposium, 199-204.

Novozhilov, V., Moghtaderi, B., Fletcher, D. F. & Kent, J. H., 1996, Fire Safety Journal, 27, 69-84.

Novozhilov, V., Harvie, D. J. E. & Kent, J. H., 1997, Fire Safety Journal, 29, 259-282.

Shiraishi, Y., Kato, S., Yoshida, S. & Murakami, S., Aug., 2001, J. Archit. Plann. Environ. Eng., AIJ, 546, 187-192.

Rouson, D. W. I., Eaton, J. K. & Abrahamson, S.D. 1997, Mech. Engng. Dept. Rep. TSD-101, Stanford University.

Tewarson, A., 1995, In The SFPE Handbook of Fire Protection Engineering, 2nd End, Ch, 3-4.

Yan, Z. H. & Holmstedt, G., 1996, Fire Safety Journal, 27, 201-238.

Yoshioka, H., Hayashi, Y., Omiya, Y., Noguchi, T., Kato, S. & Ooka, R., 2003, Summaries of Technical Papers of Annual Meeting of Architecture Institute of Japan, 117-118.